

Magnetic-field-induced evolution from electron-hole plasma to excitonic gas in photoexcited InSb

Robert D. Grober and H. Dennis Drew

*Department of Physics and Astronomy, University of Maryland, College Park, Maryland 20742
and Laboratory for Physical Sciences, College Park, Maryland 20740*

(Received 28 May 1991; revised manuscript received 5 August 1991)

We report magnetophotoluminescence spectra of undoped bulk InSb at 2 K in magnetic fields to 3.0 T. These spectra are taken at pump intensities significantly less than any previously published, comparable experiment. The zero-field, band-edge peak splits into three distinct peaks. The two high-energy peaks are due to recombination of the two lowest spin-split Landau levels. The low-energy peak is quantitatively associated with magnetoexcitons. This interpretation differs significantly from those of other magnetophotoluminescence studies of InSb and constitutes a different understanding of the relevant physics of this photoexcited system. In addition, the data suggest that the spectral position of the excitonic peak is independent of the photoexcited carrier density.

I. INTRODUCTION

There exist very few photoluminescence (PL) studies of InSb, especially in comparison to wider-band-gap III-V semiconductors. However, there are material properties unique to narrow-gap systems that make the study of InSb interesting. In particular, it has recently been documented¹ that one can photoexcite a degenerate electron-hole plasma (EHP) in insulating InSb using continuous-wave (cw) pump intensities less than 2 W/cm². The relative ease with which the EHP is generated in InSb is primarily due to the small effective electron mass ($m_c = 0.014m_0$) and large dielectric constant ($\epsilon = 16.8$) of InSb, which results in a very small Mott density ($n_c = 6 \times 10^{13}$ cm⁻³) and exciton binding energy ($E_{ex} = 0.65$ meV). In addition, InSb has a longer carrier lifetime than wider-gap III-V systems.² Using low-level pump intensities to photoexcite an EHP results in carrier temperatures not far removed from the lattice temperature.

In Ref. 1 we documented that the EHP exhibits band-gap renormalization consistent with the zero-temperature theory of Vashishta and Kalia.³ Having established the existence of a cold EHP, it is interesting to study the effects of a strong magnetic field on this system. Strong magnetic fields induce a metal-insulator transition in semiconductors doped above the Mott density. Similarly, one expects the photoexcited system to evolve from an EHP to an excitonic gas with increasing magnetic field.

In this paper we document band-edge magnetophotoluminescence (MPL) spectra of insulating InSb at 2 K in magnetic fields to 3.0 T. Similar experiments have previously been reported by several authors;⁴⁻⁷ however, we conduct this experiment at pump intensities more than an order of magnitude less than any previous experiment know to us. The resulting spectra are simpler, which makes the analysis less ambiguous. We quantitatively show that the spectra reveal a magnetic-field-induced evolution from electron-hole plasma to excitonic gas. This interpretation differs significantly from any of the

previous studies;⁴⁻⁷ however, we feel that it represents an accurate understanding of the relevant physics of photoexcited InSb in large magnetic fields.

II. EXPERIMENTAL DETAILS

We present here the PL spectra of insulating, *n*-type InSb [$n_0 = 2 \times 10^{13}$ cm⁻³ and $\mu(77$ K) = 450 000 cm²/V sec]. The details of the optical system and the method of data acquisition are described in Ref. 1. A split coil, superconducting magnet provided fields to 3.0 T. The sample and the magnet were immersed in 2 K, superfluid liquid helium throughout the experiment. The power density of the cw Nd:YAG (yttrium aluminum garnet) laser was approximately 2.0 W/cm² for the data discussed in this paper, unless otherwise stated. The experiment was done in the Voigt geometry with the magnetic field orientated in the crystallographic plane perpendicular to the [111] direction.

III. PRESENTATION OF THE DATA

Displayed in Fig. 1 are the MPL band-edge spectra for fields varying from 0 to 3.0 T. The spectra split into three distinct peaks on application of magnetic field: (1) a narrow low-energy feature, peak *a*; (2) a broad middle-energy feature, peak *b*; and (3) a weak high-energy feature, peak *c*. Peak *b* is the dominant feature at low fields. Peak *c* evolves out of the high-energy edge of the spectra. It is the weakest of the three peaks, shifts the quickest with increasing magnetic field, and is only resolvable for fields less than 1.0 T. Peak *a* evolves out of the low-energy edge of the spectra and becomes the dominant peak with increasing field. Only peak *a* is resolvable at the highest magnetic fields. The magnetic-field dependence of these peak positions are shown in Fig. 2. These data are discussed quantitatively in Sec. IV.

Shown in Fig. 3(a) is the zero-field spectrum. There are three important aspects of this spectrum, all of which are discussed in Ref. 1. First, the intensity of this spectrum

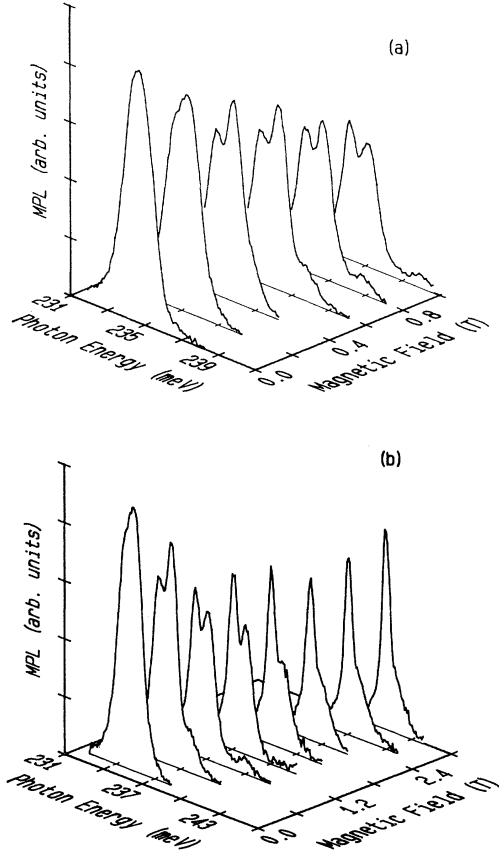


FIG. 1. Band-edge magnetophotoluminescence spectra of InSb at 2K. (a) shows spectra in magnetic fields to 1.0 T and (b) shows spectra to 3.0 T. The broad peak at zero field is peak *b*. The sharp peak that evolves out of the low-energy edge of the spectra is peak *a*. Peak *c* is on the high-energy edge of the spectra, is very weak, and can only be resolved to 1.0 T.

is proportional to the square of the pump intensity. We showed in Ref. 1 that this is consistent with a system in which optical emission is a bimolecular process but the carrier recombination is dominated by nonradiative (i.e., monomolecular) processes. Second, the spectral position of this peak decreases with increasing pump intensity.

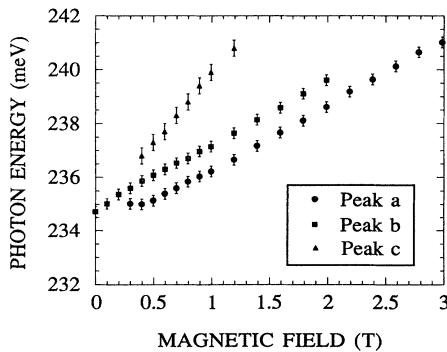


FIG. 2. Spectral positions of peaks *a*, *b*, and *c*. The error bars for peaks *a* and *b* are limited by the reproducibility of the monochromator. The error bars for peak *c* are slightly larger because this peak is fairly broad and very weak.

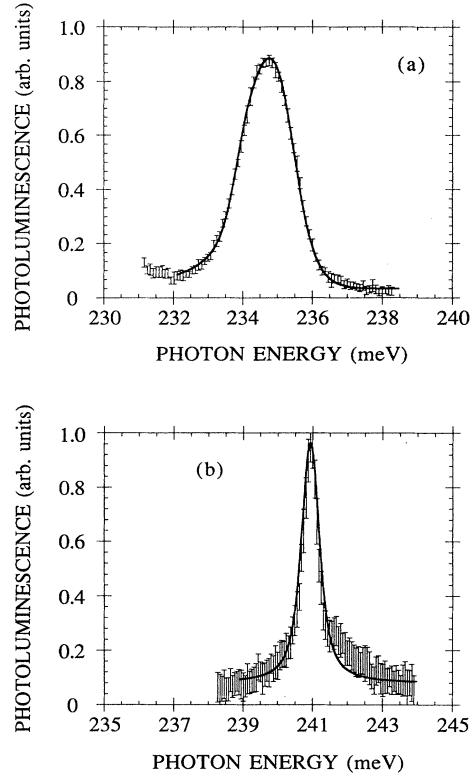


FIG. 3. Line-shape analysis of the zero-field spectrum (a) and 3.0-T spectrum (b). The solid lines correspond to the best theoretical fit. The analysis in (a) assumes recombination between free electrons and free holes. The parameters determined from this fit are $E_g = 233.7$ meV, $n = 5 \times 10^{14}$ cm $^{-3}$, and carrier temperature = 3.2 K. The fit in (b) is a Lorentzian of full width at half maximum = 0.45 meV.

This was quantitatively interpreted as band-gap renormalization of the photoexcited electron-hole plasma. Finally, the line shape can be fit using a standard interband line shape⁸

$$I_{\text{PL}}(\hbar\omega) \propto \int d^3k \int dE_e \int dE_h G_e G_h F_e F_h \times \delta(E_e - E_h - \hbar\omega), \quad (1)$$

where F_e and F_h are Fermi distribution functions, and G_e and G_h are Lorentzian spectral density functions centered at $E_{e,h} = \hbar^2 k^2 / 2m_{e,h}$. From this fit we are able to determine the renormalized band gap $E_g = 233.7$ meV, the photoexcited carrier density $n = 5 \times 10^{14}$ cm $^{-3}$, and the carrier temperature $T = 3.2$ K.

The spectrum at 3.0 T is shown in Fig. 3(b). It fits very well to a Lorentzian line shape⁹ with half-width at half maximum (HWHM) Γ of 0.22 meV. Interpreting Γ as a lifetime, $\tau = \hbar/\Gamma = 3.0$ psec agrees very well with the mobility scattering time $\tau_\mu = m_c \mu / e = 3.5$ psec, where m_c is the conduction-band mass and e is the electronic charge. The intensity of this peak increases as the square of the pump intensity. Because the HWHM of this spectrum is within a factor of 2 of the monochromator resolution, analysis of the intensity dependence of Γ does not yield meaningful results.

IV. DISCUSSION OF THE DATA

Interpretation of the PL spectra of bulk semiconductor systems are fraught with complexities. The most significant complication in InSb arises because the carriers are photoexcited at the sample surface. These carriers eventually diffuse into the sample, establishing a spatial carrier density gradient. This carrier density profile, when combined with the effects of band-gap renormalization and Fermi-level-dependent PL linewidths, can significantly complicate the spectra. Because the intensity of the PL signal is proportional to the square of the recombining carrier density, the PL emitted by the carriers nearest the sample surface dominates the spectra. For most instances this allows discussion of spectra to proceed under the assumption of a uniform photoexcited carrier density corresponding to the density nearest the sample surface. However, one must always keep in mind that distinct features in spectra could conceivably originate from different regions of the sample. When discussing such possibilities, we will only refer to two regions: (1) a high-density region near the sample surface and (2) a low-density region deeper in the sample to which few carriers have diffused.

A. Identification of peaks *b* and *c*

The realization that band-edge PL in InSb is due to the recombination of an EHP (Ref. 1) is a strong foundation on which to base the analysis of MPL spectra. One can safely assume that the EHP is quantized into Landau levels on application of a strong magnetic field. The Landau levels in InSb have been studied at length both theoretically¹⁰ and experimentally.¹¹ The first few levels are depicted schematically in Fig. 4. The labels are consistent with the formalism of Ref. 10. The dipole-allowed transitions for the lowest levels are indicated by the arrows. The band edges for the spin-up $a^c(n=0)$ and spin-down

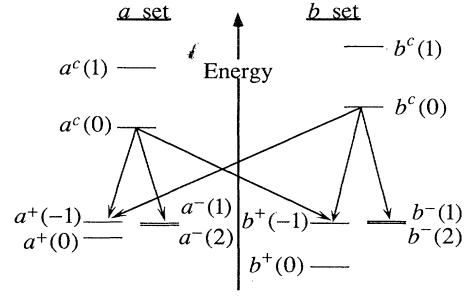


FIG. 4. A schematic of the band edges of the relevant Landau levels, as described in the text. The terminology follows that of Ref. 10. The lowest dipole-allowed transitions are shown as arrows for transitions from the spin-up $a^c(0)$ and spin-down $b^c(0)$ conduction-band Landau levels.

$b^c(n=0)$ conduction-band Landau levels are given by the model of Bowers and Yafet,¹²

$$E \begin{pmatrix} a^c(0) \\ b^c(0) \end{pmatrix} = E_g + \left[\frac{\hbar\omega_c}{2} \mp \frac{\mu g B}{2} \right], \quad (2)$$

$$\times \left[1 - \frac{\hbar\omega_c/2 \mp \mu g B/2}{E_g} \right],$$

where E_g is the zero field band gap, $\omega_c = eB/m_c c$, e is the electric charge of the electron, B is the magnetic field, c is the speed of light, μ is the Bohr magneton, and g is the effective conduction-band g -factor. Although Eq. (2) includes the first-order corrections for nonparabolicity, it is only a two percent effect even at the largest values of magnetic field used in this experiment. The band edges for the light holes, $E(a^+(n))$ and $E(b^+(n))$, and heavy holes, $E(a^-(n))$ and $E(b^-(n))$ are calculated using the quasigermanium model as summarized in Ref. 10. The expressions relevant to this experiment are

$$E \begin{pmatrix} a^+(n) \\ b^+(n) \end{pmatrix} = -\frac{eB}{2m_0 c} [(2n+3)(\gamma_1^L \mp \gamma'^L) - (2 \mp 1)\kappa^L], \quad n = -1, 0, \quad (3)$$

$$E \begin{pmatrix} a^-(n) \\ b^-(n) \end{pmatrix} = -\frac{\hbar e B}{m_0 c} \left[-\frac{(n + \frac{1}{2})\gamma_1^L \mp \gamma'^L \pm \frac{1}{2}\kappa^L \pm (\frac{5}{8} + f)q}{\{[\gamma_1^L \mp (n + \frac{1}{2})\gamma'^L - \kappa^L - \frac{1}{2}(\frac{9}{2} - f)q]^2 + 3n(n+1)(\gamma''^L)^2\}^{1/2}} \right], \quad n \geq 1, \quad (4)$$

where γ_1^L , γ'^L , γ''^L , κ^L , and q are band parameters and $f=0.25$ for a magnetic field in the crystallographic plane perpendicular to [111]. Because of the anomalous spacing of the low- n valence-band Landau levels in narrow-gap semiconductors, it is important to use the above expressions rather than the classical relation $E(B) = \hbar\omega_c(n + \frac{1}{2})$, with ω_c determined by the relevant band mass. We use the band parameters determined by Littler *et al.*¹¹ The only adjustable parameter in the calculation is the zero-field band gap E_g . We assume $E_g = 233.7$ meV, the renormalized band edge determined by line-shape analysis, and that this renormalization is in-

dependent of magnetic field. The comparison of this model with the data is shown in Fig. 5. For the theoretical lines labeled spin up, the solid line corresponds to the $a^c(0) \rightarrow a^-(1)$ transition, the long-dashed line corresponds to $a^c(0) \rightarrow a^+(-1)$, and the short-dashed line corresponds to $a^c(0) \rightarrow b^+(-1)$. Similarly for the lines labeled spin down, the solid line corresponds to the $b^c(0) \rightarrow b^-(1)$ transition, the long-dashed line corresponds to $b^c(0) \rightarrow b^+(-1)$, and the short-dashed line corresponds to $b^c(0) \rightarrow a^+(-1)$. Note that the data points indicate the position of the peak of the particular feature.

The following issues concerning the results shown in

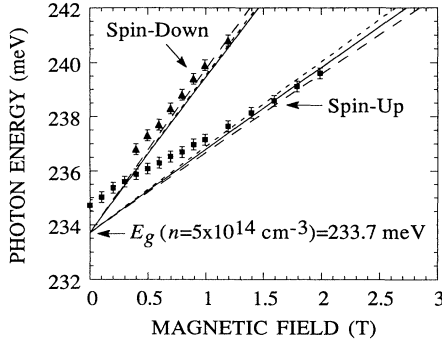


FIG. 5. A comparison of peak *b*, shown as the square boxes, and peak *c*, shown as the triangles, with the theoretical band edges for the six dipole-allowed interband transitions from the two lowest, spin-split, conduction-band Landau levels. The transitions are identified in the text.

Fig. 5 are discussed below: (1) the peak positions move closer to the theoretical band edges as the magnetic field increases, and (2) there is good agreement between theory and experiment in the large-field limit even though a magnetic-field-independent renormalization energy is assumed.

The first issue is easily understood in terms of the electron density of states. In the absence of a magnetic field, the density of states is proportional to $(E - E_g)^{1/2}$ (i.e., the density of states increases as one gets further from the band edge). The resulting PL spectra peaks at an energy greater than the band edge, as seen in Fig. 3(a). This spectrum can be understood roughly as the convolution of the density of states with the appropriate Fermi functions. On the other hand, the density of states in a strong magnetic field goes as $\{1/[E - E_g(B)]\}^{1/2}$, where $E_g(B)$ is the magnetic-field-dependent band edge (i.e., the peak of the density of states occurs at the band edge). In the strong-field limit the peak of the MPL spectra should occur very near the actual band edge. In practice, one expects the MPL peak to move towards the band edge with increasing magnetic field. This is clearly seen in Fig. 5.

One might expect the renormalization energy to be dependent on the magnetic field for the following reasons: (1) With increasing magnetic field the electron population statistics change from degenerate to nondegenerate. This most significantly affects the exchange energy. (2) As shown in the next section, the system evolves from EHP to excitonic gas with increasing magnetic field. Assuming excitons are not as effective at screening as are free carriers, effects due to screening should decrease as the number of free carriers decrease. Nonetheless, the experimental results indicate that the renormalization energy is not strongly dependent on magnetic field. Although a precise calculation is beyond the scope of this paper, we can estimate the size of the renormalization in the large-field limit by calculating the static limit of the Coulomb-hole self-energy,¹³ $E_{ch} = \sum_k [V_s(k) - V(k)] = -(e^2/\epsilon)k_s$, where V_s is the statically screened Coulomb potential and k_s is the screening wave vector. From the work in Ref. 1, we know PL becomes unobservable at carrier densities of

the order of $5 \times 10^{13} \text{ cm}^{-3}$. Using the large-field limit of k_s , as determined by Horing,¹⁴ a carrier density of $5 \times 10^{13} \text{ cm}^{-3}$, and a carrier temperature of 3.2 K, we determine $E_{ch} = -1.2 \text{ meV}$. This of the same order of magnitude as the zero-field renormalization. Thus, it is not improbable that the renormalization energy is weakly dependent on magnetic field.

In summary, we attribute peaks *b* and *c* to the recombination of electrons with holes quantized in the lowest Landau levels. This recombination is not excitonic. It involves transitions between free electrons and free holes.

B. Identification of peak *a*

Historically, this peak has been attributed to recombination of either a magnetic-field stabilized electron-hole liquid^{4,5} or impurity bound magnetoexcitons.^{6,7} Both of these assignments were biased by the incorrect assumption that peak *b* is due to the recombination of free magnetoexcitons.

In what follows, we explore and subsequently reject the notion that peak *a* is attributable to an electron-hole liquid. For completeness, amplified spontaneous emission is also eliminated as a possible explanation. Finally, we show quantitatively that peak *a* is associated with recombination of free magnetoexcitons.

1. Electron-hole liquid

The minimal conditions necessary for EHL condensation¹⁵ require that the temperature of the electronic system be less than some critical temperature T_c . This temperature is roughly given by the relation $kT_c = 0.1E_{ex}$ resulting in $T_c = 0.7 \text{ K}$ for InSb, more than a factor of 4 less than the 3.2 K carrier temperature. Even in magnetic fields where the excitonic Rydberg increases dramatically, T_c should not become as large as 3.2 K until the field strength becomes approximately 0.8 T.¹⁶ However, this low-energy feature is resolved at fields as low as 0.3 T. These energetic arguments render EHL condensation unlikely.

The most compelling reason to rule out EHL is the spectra itself. Thomas *et al.*¹⁷ have thoroughly documented the PL spectra of EHL. The characteristic spectrum consists of two peaks: (1) a narrow high-energy feature due to exciton recombination, and (2) a broad low-energy feature due to the EHL. The width of the low-energy feature is determined by the Fermi energy of the EHL equilibrium carrier density. The separation in energy between these two features corresponds to the EHL binding energy. The spectra reported in this experiment are exactly opposite to the spectra of Thomas *et al.* Peak *b*, the high-energy peak, is fairly broad while peak *a*, the low-energy peak, is very narrow.

Therefore, we rule out EHL condensation as the mechanism responsible for peak *a*.

2. Amplified spontaneous emission

Photoluminescence line shape is given by the general formula

$$S(\hbar\omega) = \sum_{k,\sigma} R_{sp}(\hbar\omega) [1 + N_{k,\sigma}(\hbar\omega_{k,\sigma})] \delta_{\omega\omega_{k,\sigma}}, \quad (5)$$

where the summations are over the photon modes. $R_{sp}(\hbar\omega)$ is determined uniquely by the electronic band structure and the carrier statistics. $N_{k,\sigma}(\hbar\omega)$, the number of photons in the optical mode specified by wave number k and helicity σ , is usually assumed less than unity. This renders the PL spectra dependent only on the electronic properties of the sample. When photon modes become macroscopically occupied, amplified spontaneous emission (ASE) becomes relevant and $N_{k,\sigma}(\hbar\omega)$ significantly alters the PL line shape. To correctly interpret the PL spectra, one must determine whether the photon density has an appreciable effect on the spectral line shape.

The position of the low-energy feature is an immediate reason to rule out ASE. Since there is no resonant cavity, the onset of ASE should occur at the maximum of the gain spectra. This is clearly not the case for peak a . Making a more quantitative statement, we estimate that the photon density detected in our PL measurement is between 10^{-3} and 10^{-2} photons/mode. This is consistent with the experiments of Kalugina and Stork⁵ where it was documented that the onset of stimulated emission in InSb occurs at a pump photon flux of 10^{22} photons/cm² sec, approximately 10^3 times greater than that used in this study.

For these reasons, we rule out ASE as an explanation of peak a .

3. Magnetoexcitons

Qualitatively, the separation in energy between peaks a and b suggest that peak a is a weakly bound state just below the band edge. The line shape of peak a further suggests a bound system. Two possibilities for such a state are either donor bound electrons or excitons. Exciton and donor PL should be spectrally indistinguishable because the ratio of m_c to the heavy-hole mass is approximately 30. However, exciton PL should dominate donor PL in this experiment because the number of photoexcited holes is several times larger than the number of donors.¹⁸ For this reason, we phrase the following analysis in the language of excitons.

One can model the magnetoexciton as a hydrogen atom in a strong magnetic field.¹⁹ The Schrödinger equation for this system is

$$-\nabla^2\Psi + \gamma L_z\Psi + \gamma^2(x^2 + y^2)\Psi - \frac{2}{r}\Psi = E\Psi, \quad (6)$$

where all lengths are normalized to the exciton Bohr radius $a_{ex} = \hbar^2\epsilon/e^2m^*$, m^* is the reduced mass of the electron-hole system, all energies are normalized to the exciton Rydberg $E_{ex} = \hbar^2/2m^*a_{ex}^2$, and $\gamma = \hbar\omega_c/2E_{ex}$ is the ratio of the cyclotron energy to twice the exciton Rydberg. Experimental realization of the high-field ($\gamma \gg 1$) regime in InSb is not very difficult. For example, a magnetic field of 1.0 T corresponds to $\gamma = 6.3$. Equation (6) neglects any nonparabolicity effects of the conduction band and any effects due to the complicated valence-band structure. Neglecting nonparabolicity is reasonable since it was shown above that nonparabolicity is at most a two percent effect. Analytical solutions to Eq. (6) do not yet exist.

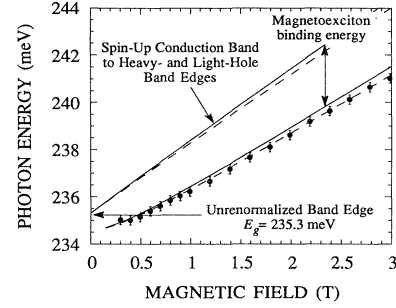


FIG. 6. A comparison of peak a , shown as the solid circles, with the theoretical positions of the magnetoexcitons associated with the $a^c(0) \rightarrow a^-(1)$ and $a^c(0) \rightarrow a^+(-1)$ transitions. The exciton binding energy is calculated using the method of Ref. 20. The unrenormalized band edges are shown for reference. The data correlates most closely with the $a^c(0) \rightarrow a^+(-1)$ transition.

Of particular importance to this experiment is the ground-state binding energy, $E_{ex}(B)$. We use the results of Larsen²⁰ to determine $E_{ex}(B)$. This method provides a relatively easy formalism with which to calculate the binding energies. A recent paper by Trzeciakowski *et al.*²¹ compared the model of Larsen with more complete numerical models and showed that energies calculated using Larsen's wave functions are correct to better than 1% for magnetic fields as large as $\gamma = 20$.

To compare these calculations with the experimental data one must first determine from where to measure the binding energy. If the excitons exist only in the low-density region of the sample the binding energy must be measured from the unrenormalized band edge. If the excitons exist in the high-density region, both band-gap renormalization and screening of the magnetoexciton need to be considered. Haug and Schmitt-Rink¹³ have shown that for bulk systems the spectral position of the exciton is remarkably constant as a function of electron-hole pair density. They comment that this reflects the charge neutrality of the exciton. Their calculation does not consider the effects of an external magnetic field. Rezayi and MacDonald²² recently showed that this cancellation is an exact result in two-dimensional systems, even in large magnetic fields. Thus, it is not without precedent to expect that the many-body magnetoexciton may be treated as an unscreened system. We calculate the position of the magnetoexciton emission energy as follows: (1) Assume an unscreened band gap of $E_g = 235.3$ meV, consistent with our results in Ref. 1 and the comprehensive results of Littler *et al.* (2) Calculate the two lowest a -set transitions, $a^c(0) \rightarrow a^-(1)$ and $a^c(0) \rightarrow a^+(-1)$. (3) Subtract from these transition energies the magnetoexciton binding energy as determined by the calculation of Larsen. The results of this calculation are compared with the experimental peak positions in Fig. 6. The experimental points correlate very strongly with the $a^c(0) \rightarrow a^+(-1)$ excitonic transition. However, the theoretical splitting between the $a^c(0) \rightarrow a^-(1)$ and $a^c(0) \rightarrow a^+(-1)$ transition is only 0.25 meV, which is comparable to both the spectral linewidth and the accuracy with which one can

claim to know E_g . It is thus unlikely that we can actually distinguish between these two transitions. Nonetheless, this analysis provides quantitative evidence that peak a is related to the recombination of free magnetoexcitons.

V. DISCUSSION OF THE RESULTS

Quantitative analysis of the spectral position of peak a strongly suggests that it is an excitonic state. The Lorentzian line shape also implies a bound system. That the lifetime inferred from the width of the peak correlates well with the mobility scattering lifetime is consistent with the picture of a free exciton.

Peak a increases as the square of the pump intensity. This too can be shown to be consistent with exciton emission by considering the following simple rate equation analysis. Assume that photoexcitation generates carriers far above the band edge. After many collisions the electrons and holes relax to the band edge as uncorrelated entities. To form an exciton an electron and hole must find one another. This is proportional to both density of electrons and the density of holes. Thus we define a bimolecular exciton generation rate $r_{\text{ex}}n^2$. Once formed, the exciton optical recombination rate is monomolecular²³ with lifetime τ_{ex} . The rate equation for the exciton is given as

$$\frac{\partial n_{\text{ex}}}{\partial t} = -\frac{n_{\text{ex}}}{\tau_{\text{ex}}} + r_{\text{ex}}n^2. \quad (7)$$

The steady-state solution yields the relation $n_{\text{ex}} \propto n^2$. One must now consider the density of electrons. As was shown in Ref. 1, the rate equation in steady state is

$$\frac{\partial n}{\partial t} = I_p - \frac{n}{\tau_{\text{nr}}} - rn^2 - r_{\text{ex}}n^2 = 0, \quad (8)$$

where τ_{nr} is the nonradiative recombination lifetime and r is the bimolecular radiative recombination coefficient. Since the carrier recombination in InSb is dominated by nonradiative processes (see Sec. III), the relation between electron density and pump intensity is $n \propto I_p$. Therefore, the exciton luminescence intensity is given as $w_{\text{ex}} \propto n_{\text{ex}} \propto n \propto 2 \propto I_p^2$, which is consistent with the experimental observation.

The carriers photoexcited by the optical pump diffuse into the sample establishing a spatial carrier density gradient. One must be concerned as to whether this exciton exists in the high carrier density region near the sample surface or in a lower density region deeper in the sample. The answer lies in the fact that the intensity of exciton PL is proportional to the density of excitons, which is proportional to the square of the free carrier density. Thus, exciton PL from the low-density region should be weak in comparison to PL from the high-density region. Therefore, we presume that peak a originates in the high-density region.

The identification of peak a as recombination of magnetoexcitons requires that there be an exact cancellation between band-gap renormalization and screening of the exciton for this three-dimensional system in large magnetic fields. To the best of our knowledge this has not yet been shown theoretically. To test this idea further we studied the spectral position of peak a for pump intensi-

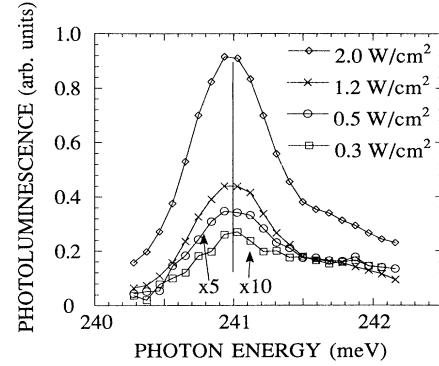


FIG. 7. MPL pump intensity dependence at 3.0 T. The spectra for 0.5 and 0.3 W/cm² have been scaled by factors of 5 and 10, respectively. These spectra were recorded with 500- μm slits, as opposed to the 250- μm slits used for the spectra of Fig. 3(b), and therefore appear slightly broader. The larger slit was necessary to improve sensitivity for the spectra taken at low pump intensity.

ties ranging from 0.3 to 2 W/cm², in magnetic fields ranging from 1.0 to 3.0 T, with experimental resolution to ± 0.1 meV. Spectra taken at 3.0 T are shown in Fig. 7. We do not observe any measurable shift in the position of peak a by varying the pump intensity. This suggests that the identity found by Rezayi and MacDonald for two-dimensional systems may also exist for three-dimensional systems.

Another interesting issue raised by our interpretation of peak a concerns the magnetic-field-induced metal-insulator transition. For n -type semiconductors doped above the Mott density, there exists some critical field B_c at which the system undergoes a metal-insulator transition (MIT). This transition has been studied in InSb (Ref. 24) and was found to be described by the equation $na_{\perp}^2 a_{\parallel} = (0.22)^3$, where a_{\perp} and a_{\parallel} are parameters of the hydrogenic wave function of Yafet, Keyes, and Adams.²⁵ For a donor density of $5 \times 10^{14} \text{ cm}^{-3}$, InSb should have a metal-insulator transition at 1.0 T. Similar arguments should be applicable to the exciton when EHL concepts are not relevant. It is intriguing that we resolve excitons at magnetic fields as low as 0.3 T. Optical evidence for bound states on the metallic side of the MIT has recently been documented by Choi and Drew²⁶ in both InSb and $\text{Hg}_{1-x}\text{Cd}_x\text{Te}$ and by Romero *et al.*²⁷ in GaAs. In these far-infrared experiments impurity cyclotron resonance (ICR) is observed at fields significantly less than B_c . The field at which the onset of ICR is observed corresponds to B_c for a system with a carrier density five times smaller than the actual system. This is consistent with our observations. InSb with a carrier density of $n = 1 \times 10^{14} \text{ cm}^{-3}$ should undergo a MIT at $B_c = 0.3$ T. Our experiment suggests that MPL studies specifically designed to probe the MIT could provide additional insight into the nature of this transition.

VI. CONCLUSION

We report magnetophotoluminescence spectra of undoped bulk InSb at 2 K in magnetic fields to 3.0 T. The

zero-field band-edge peak is observed to split into three distinct peaks. The two higher-energy peaks are identified as recombination radiation of the lowest spin-split conduction-band Landau levels. The low-energy peak is quantitatively identified as recombination radiation of magnetoexcitons. This interpretation differs significantly from any previous interpretation of MPL in InSb and constitutes the first time such data has had a

quantitative explanation. Finally, our data suggest that the spectral position of the magnetoexciton is independent of the photoexcited electron-hole pair density.

ACKNOWLEDGMENTS

We would like to thank Dr. Marvin Kruger and Dr. William Johnson for valuable discussions.

- ¹R. D. Grober and H. D. Drew, Phys. Rev. B **43**, 11 732 (1991).
²H. J. Fossum and B. Ancker-Johnson, Phys. Rev. B **8**, 2850 (1973).
³P. Vashishta and R. K. Kalia, Phys. Rev. B **25**, 6492 (1982).
⁴I. V. Kavetskaya, Ya. Ya. Kost', N. N. Sibel'din, and V. A. Tsvetkov, Pis'ma Zh. Eksp. Teor. Fiz. **36**, 254 (1982) [JETP Lett. **36**, 311 (1982)].
⁵N. A. Kalugina and E. M. Stork, Pis'ma Zh. Eksp. Teor. Fiz. **38**, 251 (1983) [JETP Lett. **38**, 297 (1983)]; Fiz Tverd. Tela (Leningrad) **27**, 528 (1985) [Sov. Phys. Solid State **27**, 324 (1985)].
⁶V. I. Ivanov-Omskii *et al.*, Fiz. Tekh. Poluprovodn. **7**, 532 (1983) [Sov. Phys. Semicond. **17**, 334 (1983)]; R. P. Seisyan and Sh. U. Yuldashev, Fiz. Tverd. Tela (Leningrad) **30**, 12 (1988) [Sov. Phys. Solid State **30**, 6 (1988)].
⁷I. V. Kavetskaya and N. N. Sibel'din, Pis'ma Zh. Eksp. Teor. Fiz. **38**, 67 (1983) [JETP Lett. **38**, 76 (1983)].
⁸M. Capizzi, S. Modesti, A. Frova, J. L. Staehli, M. Guzzi, and R. A. Logan, Phys. Rev. B **29**, 2028 (1984).
⁹The spectra is actually fit to a convolution of a Lorentzian with a Gaussian. The Gaussian is used to model the monochromator instrument function. It is determined by dispersing a Nd:YAG laser into the monochromator, measuring the line shape of the fifth-order diffraction (i.e., the diffraction that occurs closest in wavelength to the actual luminescence spectra), and fitting that spectrum to a Gaussian line shape. For the spectra in Fig. 3(b), which was taken with 250- μm slits, the standard deviation of the Gaussian instrument function was 0.13 meV.
¹⁰For a review, see M. H. Weiler, in *Semiconductors and Semimetals*, edited by R. K. Willardson and A. C. Beer (Academic, New York, 1981), Vol. 16, p. 119.
¹¹See, for example, C. L. Littler, D. G. Seiler, R. Kaplan, and R. J. Wagner, Phys. Rev. B **27**, 7473 (1983).
¹²R. Bowers and Y. Yafet, Phys. Rev. **115**, 1165 (1959).
¹³H. Haug and S. Schmitt-Rink, Prog. Quantum Electron. **9**, 3 (1984).
¹⁴N. H. Horing, Ann. Phys. **54**, 405 (1969).
¹⁵L. V. Keldysh, Contemp. Phys. **27**, 395 (1986).
¹⁶This is based on the assumption that the critical temperature scales as the magnetoexciton binding energy. The magnetic-field dependence of the exciton binding energy is discussed in Sec. IV B 3.
¹⁷G. A. Thomas *et al.*, Phys. Rev. Lett. **31**, 386 (1973); G. A. Thomas, T. M. Rice, and J. C. Hensel, *ibid.* **33**, 219 (1974).
¹⁸We estimate that the number of compensating acceptors p_a in this sample is less than $1 \times 10^{14} \text{ cm}^{-3}$. Since the number of photoexcited carriers is $5 \times 10^{14} \text{ cm}^{-3}$, the ratio of valence-band holes p to bound acceptors should be $p/p_a > 4$.
¹⁹R. J. Elliott and R. Loudon, J. Phys. Chem. Solids **15**, 196 (1960).
²⁰D. M. Larsen, J. Phys. Chem. Solids **29**, 271 (1968).
²¹W. Trzeciakowski *et al.*, Phys. Rev. B **33**, 6846 (1986).
²²E. H. Rezayi and A. H. MacDonald, Bull. Am. Phys. Soc. **36**, 915 (1991).
²³H. H. Bebb and E. W. Williams, *Semiconductors and Semimetals* (Academic, New York, 1972), Vol. 8, Chap. 4.
²⁴M. Shayegan *et al.*, Phys. Rev. B **32**, 6952 (1985).
²⁵Y. Yafet, R. W. Keyes, and E. N. Adams, J. Phys. Chem. Solids **1**, 137 (1956).
²⁶J. B. Choi and H. D. Drew, Phys. Rev. B **41**, 8229 (1990).
²⁷D. Romero *et al.*, Phys. Rev. B **42**, 3179 (1990).